Thermocharge of a hot spot in an electrolyte solution

Arghya Majee, Alois Würger

Thermocharge of a hot spot in an electrolyte solution

Arghya Majee and Alois Würger
Laboratoire Ondes et Matière d'Aquitaine, Université Bordeaux 1 & CNRS, 351 cours de la Libération, 33405 Talence, France

We discuss the thermoelectric properties of a locally heated micron-size volume in an electrolyte solution. We find that such a hot spot carries a net charge Q which, for an excess temperature of 10 K, may attain hundreds of elementary charges. The corresponding Seebeck electric field E increases linearly with the radius r inside the heated area, then goes through a maximum, and decays as $1/r^2$ at larger distances. Our results could be relevant for optothermal actuation of electrolytes and colloidal suspensions.

PACS numbers: 66.10.C, 82.70.-y,47.57.J-

I. INTRODUCTION

Heating a micron-size domain by a focussed laser beam has become a standard technique of optothermal actuation in microfluidics. Thus a DNA trap was realized through a thermal barrier in a microchannel [1] and the droplet size of a thermocapillary valve has been shown to be sensitive to the Marangoni effect [2]. In a thin aqueous film, Soret-driven depletion of polymers from a hot spot can be used for confining 100 nm colloidal beads to a micro-domain [3], or for separating solutes like RNA by size [4]. As a recent biotechnological application, protein interactions in biological liquids were studied by microscale thermophoresis [5].

The underlying thermal forces depend on the applied temperature gradient through various mechanisms that are not always easily separated [6–8]. The common physical picture relies on local effects such as thermoosmosis around solute particles [9], or Marangoni forces along fluid interfaces [10]; molecular-dynamics simulations suggest that even the molecular orientation, in both polar and non-polar liquids, is sensitive to a temperature gradient [11, 12]. In recent years it has become clear that, for charged systems in an electrolyte solution, the thermoelectric or Seebeck effect provides a non-local driving force that presents surprising properties.

In a non-uniform temperature, positive and negative salt ions have a tendency to migrate in opposite directions, thus giving rise to a thermopotential between the hot and cold boundaries of the sample [13–15], and to a thermoelectric field $E = S\nabla T$ that is proportional to the temperature gradient. In a colloidal suspension, this field drives the solute particles at a velocity $u = \mu E$, where μ is the Helmholtz-Smoluchowski electrophoretic mobility. The Seebeck coefficient S depends on the electrolyte and may take either sign; the resulting reversal of the drift velocity has been observed experimentally for colloidal particles [16] and SDS micelles [17], upon replacing NaCl ($S > 0$) by sodium hydroxide NaOH ($S < 0$). A detailed comparison showed that the Seebeck effect dominates the thermoosmotic pressure of mobile ions in the electric double layer of the colloid [18]. Moreover, it was found [19] that the thermoelectric effect is at the origin of

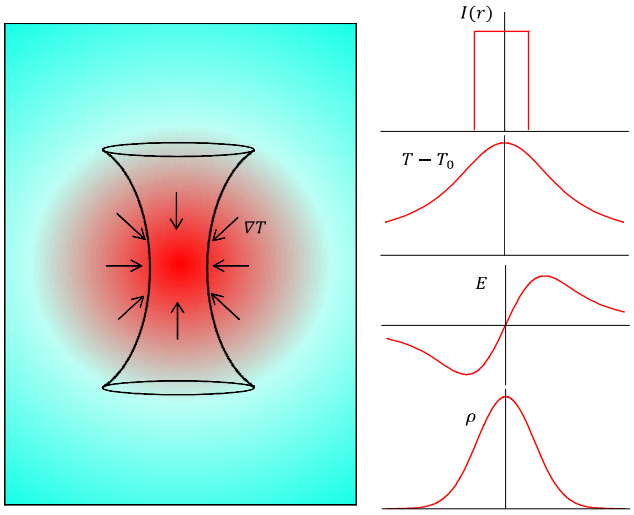

FIG. 1: Schematic view of a micron-size volume heated by absorption of a focussed laser beam in an electrolyte solution. The right panel compares the heating power $I(r)$ with the excess temperature $T - T_0$, the thermoelectric field E, and the net charge density ρ.

the observed dependence of the mobility on the colloidal volume fraction [20], and on the molecular weight of polyelectrolytes [21] and DNA [22]. The recently reported non-uniform variation of the Soret coefficient with the ionic strength [23] is characteristic for the electrophoretic mobility [24, 25] and thus confirm the relevance of the Seebeck effect for the colloidal motion. The examples cited so far concern a one-dimensional geometry, where a constant temperature gradient arises from heating one side of the sample and cooling the opposite side [26, 27]. Because of the macroscopic volume, boundary effects and in particular the surface charges at the cold and hot walls are negligible.

The present paper studies the thermoelectric properties of a locally heated micron-sized volume in a bulk liquid, and discusses the ensuing colloidal transport. The three-dimensional geometry results in a non-uniform thermoelectric field and a net charge that is concentrated

in the hot spot. The present work is complementary to our recent study of the thermoelectric properties of a heated colloidal particle [28], where the spatial separation of the heated volume (inside the bead) and the area where mobile ions are present (outside) significantly simplified the problem.

Here we consider the thermoelectric properties of a hot spot in a bulk liquid. The simple example of a square absorption profile is shown in Fig. 1. The excess temperature is a smooth function within the heated area and decays with the inverse distance outside. Thermodiffusion of the mobile ions induces a thermoelectric field that follows roughly the temperature gradient, and is related to a net thermocharge confined within the heated area. Since the salt ions diffuse within the waist of the focussed laser beam, the electrostatic and thermal equations have to be solved simultaneously. In Section 2 we present the general solution of the electrolyte Seebeck effect in a non-uniform temperature. The case of a Gaussian profile of the laser intensity is discussed in Section 3, and simplified for the most relevant situation where the Debye length is small as compared to the size of the heated area. Section 4 is devoted to colloidal transport. In Sects. 5 and 6 we discuss the validity of the approximations made and summarize our main results.

II. ELECTROLYTE SEEBECK EFFECT

Suppose we have an electrolyte solution in a container and we are heating a small region of this solution by a focused laser beam. The absorbed power density βI is determined by the laser intensity $I(\mathbf{r})$ and the optical absorption coefficient β. Then the temperature profile is solution of the stationary limit of Fourier's equation $\kappa\boldsymbol{\nabla}^2 T + \beta I = 0$, where κ is the heat conductivity. Its formal solution reads

$$T(\mathbf{r}) - T_0 = \frac{\beta}{\kappa}\int dV' \frac{I(\mathbf{r}')}{|\mathbf{r}-\mathbf{r}'|}. \tag{1}$$

Throughout this paper we consider an isotropic intensity, though in experiments the transverse and longitudinal dimensions of the focus volume in general differ from each other.

The bell-shaped temperature profile results in a thermal gradient that is zero at the center of the heated spot, takes a maximum at its border, and then decays with distance as $1/r^2$. As a consequence of this temperature gradient, the mobile ions of the electrolyte solution will start moving. We briefly present the underlying physical mechanisms and then discuss the steady-state thermoelectric field.

A. Ion thermodiffusion

We consider a monovalent electrolyte solution of ionic strength n_0 and non-uniform temperature T. Then the ion currents consist of three terms [8, 14, 15],

$$\mathbf{J}_\pm = -D_\pm\left(\boldsymbol{\nabla} n_\pm + 2\alpha_\pm n_\pm \frac{\boldsymbol{\nabla} T}{T}\right) \pm \mu_\pm n_\pm e\mathbf{E}, \tag{2}$$

where the first one corresponds to gradient diffusion with Einstein coefficients $D_\pm$, the second accounts for thermal diffusion with the dimensionless Soret parameters $\alpha_\pm$, and the last term describes electrophoresis in the electric field $\mathbf{E}$ with the Hückel mobility $\mu_\pm$ of monovalent ions. For ions of radius much smaller than the Debye length, these coefficients are related through [29]

$$D_\pm = \mu_\pm k_B T. \tag{3}$$

Eq. (2), which arises in Onsager's theory for irreversible processes, describes various non-equilibrium situations, depending whether the concentration gradient, the temperature gradient, or the electric field are taken as the external driving force [31]. As a well-known example, we mention the case of an external salinity gradient $\boldsymbol{\nabla} n_\pm \neq 0$ with uniform temperature $\boldsymbol{\nabla} T = 0$: Unlike Einstein coefficients of positive and negative ions lead to a diffusion electric field $E \propto D_+ - D_-$ and a "chemiphoretic effect" [30].

Here we are interested in the Seebeck effect, which establishes the relation between an applied temperature gradient and the resulting thermoelectric field E. As source strength we have introduced the ionic Soret parameters $\alpha_\pm$ that are given by the ratio of thermodiffusion and diffusion coefficients. The above definition implies that ions with positive $\alpha_\pm$ migrate to the cold. In view of the early literature on non-uniform salt solutions, these parameters may be considered as a dimensionless measure of Eastman's "entropy of transfer" $S^*_\pm = 2\alpha_\pm k_B$ [13] and Agar's "heat of transport" $Q^*_\pm = 2\alpha_\pm k_B T$ [15]. In physical terms, the $\alpha_\pm$ are determined by the ionic solvation free energy, which is a complex function of electrostatic and hydration forces; at present there is no satisfactory theoretical description for these parameters. From the osmotic pressure of an ideal gas one obtains $\alpha_\pm = 1$. For common monovalent salt ions these numbers vary between 0 and 1 [18]; larger values occur for molecular ions containing hydrogen.

B. Steady state

We discard transients due to an initial out-of equilibrium state. The steady state is achieved if different contributions to the ion currents (2) cancel each other,

$$\mathbf{J}_\pm = 0. \tag{4}$$

We briefly discuss the case where the thermodiffusion parameters are identical $\alpha_+ = \alpha_-$. Then the electric field vanishes, and cations and anions show the same concentration modulation $n_\pm = n_0$. The non-uniform salinity is described by $\boldsymbol{\nabla} n_0 = -n_0 S_T \boldsymbol{\nabla} T$ with the salt Soret

coefficient $S_T = (\alpha_+ + \alpha_-)/T$. Note that this "Soret equilibrium" involves diffusion and thermodiffusion contributions to (2) only, and thus implies $E = 0$.

Now we turn to the electrolyte Seebeck effect that arises from the difference $\alpha_+ - \alpha_-$ of the single-ion Soret parameters. Then the steady state condition (4) cannot be achieved with the same concentration profile for positive and negative ions. In other words, there is a finite charge density

$$\rho = e(n_+ - n_-),$$

which in turn is related to an electric field. Mechanical equlibrium is obtained where the thermodynamic and Coulomb forces cancel each other. The steady-state electric field and charge distribution are related through Gauss' law

$$\boldsymbol{\nabla} \cdot \mathbf{E} = \rho/\varepsilon. \tag{5}$$

C. Linearization

The conditions (4) and (5) determine the stationary thermoelectric properties of the heated spot. Subtracting the equations $\mathbf{J}_\pm/D_\pm = 0$ from each other, and introducing the gradient of charge density $\boldsymbol{\nabla}\rho$ we get

$$\boldsymbol{\nabla}\rho + 2e(n_+\alpha_+ - n_-\alpha_-)\frac{\boldsymbol{\nabla}T}{T} - (n_+ + n_-)\frac{e^2\mathbf{E}}{k_BT} = 0. \tag{6}$$

This intricate non-linear relation for the quantities $n_\pm$ simplifies significantly when resorting to a linearization approximation in terms of the out-of-equilibrium quantities, that is, the excess temperature, and the resulting density changes and thermoelectric field. This amounts to replacing, in the coefficients of $\boldsymbol{\nabla}T$ and $\mathbf{E}$, the temperature T and the ion densities $n_\pm$ with their bulk mean values T_0 and n_0. Note that we keep the density gradient in the first term.

Thus the linearization approximation does not require small gradients $\boldsymbol{\nabla}n_\pm$ but relies on the weaker conditions

$$\delta T \ll T_0, \qquad |n_\pm - n_0| \ll n_0. \tag{7}$$

Retaining the gradient $\boldsymbol{\nabla}\rho$ but neglecting corrections in the excess temperature $\delta T/T_0$ and the modulation of ion densities $n_\pm/n_0 - 1$, Eq. (6) simplifies to

$$\boldsymbol{\nabla}\rho + 2en_0(\alpha_+ - \alpha_-)\frac{\boldsymbol{\nabla}T}{T_0} - 2n_0\frac{e^2\mathbf{E}}{k_BT_0} = 0. \tag{8}$$

In the following we determine the Seebeck field E from a set of two coupled equations, which are Gauss' law (5) and the linearized thermoelectric relation (8).

D. Thermoelectric field

Defining the Debye length $\lambda = (\varepsilon k_BT_0/2e^2n_0)^{1/2}$ and the Seebeck coefficient

$$S = \frac{k_B}{e}(\alpha_+ - \alpha_-),$$

TABLE I: Seebeck coefficient S for NaCl, HCl, NaOH, and tetrabutylammonium nitrate (TBAN) in aqueous solution [15, 32, 33]. The Seebeck coefficient is given by the difference of the reduced single-ion Soret coefficients, $S = (k_B/e)(\alpha_+ - \alpha_-)$. The dimensionless parameters $\alpha_\pm$ are related to the "heat of transfer" $Q^*_\pm = 2k_B\alpha_\pm$. For comparison, the Seebeck coefficient of most simple metals is of the order of a few μV/K.

Salt	NaCl	NaOH	HCl	TBAN
S (mV/K)	0.05	−0.22	0.21	1.0
$\alpha_+ - \alpha_-$	0.6	−2.7	2.6	12

we then obtain the equation for the electric field

$$\mathbf{E} = \lambda^2\frac{\boldsymbol{\nabla}\rho}{\varepsilon} + S\boldsymbol{\nabla}T.$$

This form shows that the electric field consists of two contributions: one is related to the gradient of the charge density and the other one is proportional to the temperature gradient. Inserting Gauss' law in the first one, we get an inhomogeneous linear equation for the electric field:

$$\lambda^2\boldsymbol{\nabla}(\boldsymbol{\nabla}\cdot\mathbf{E}) - \mathbf{E} + S\boldsymbol{\nabla}T = 0. \tag{9}$$

In order to avoid the vector derivatives, we insert $\mathbf{E} = -\boldsymbol{\nabla}\varphi$ and obtain the corresponding equation for the electrostatic potential,

$$\lambda^2\boldsymbol{\nabla}^2\varphi - \varphi = S(T - T_0), \tag{10}$$

where the constant T_0 gives the temperature far from the heated spot. This is identical to the usual Debye-Hückel equation, albeit with the source field $S(T - T_0)$. Since we consider an infinite bulk liquid without internal boundaries, the formal solution of (10) is readily obtained as the convolution of the screened propagator $g(\mathbf{r}') = e^{-r'/\lambda}/4\pi r'\lambda^2$ with the temperature profile,

$$\varphi(\mathbf{r}) = -S\int dV' g(\mathbf{r}')(T(\mathbf{r} - \mathbf{r}') - T_0). \tag{11}$$

The thermoelectric field is calculated by taking the gradient,

$$\mathbf{E}(\mathbf{r}) = S\int dV' g(\mathbf{r}')\boldsymbol{\nabla}T(\mathbf{r} - \mathbf{r}'). \tag{12}$$

The thermoelectric field originates from the charge density $\rho = \varepsilon\boldsymbol{\nabla}\cdot\mathbf{E}$ accumulated in the heated spot by the thermodiffusion current. The total charge is obtained by integrating over volume,

$$Q = \int dV\rho.$$

Because of the overall neutrality, there is a countercharge $-Q$ at infinity or, in the case of a finite system, at the sample container.

E. Smooth temperature profile

The size a of the heated spot is at least of the order of microns, and more often of tens of microns. Except for very weak electrolytes, this is significantly larger than the Debye length λ; thus to leading order in λ/a, the function $g(\mathbf{r}')$ can be replaced with Dirac's delta peak $\delta(\mathbf{r}')$. More generally, this approximation is valid as long as the temperature profile varies little over one Debye length.

Then the thermopotential is proportional to the excess temperature, $\varphi_0(\mathbf{r}) = -S(T(\mathbf{r}) - T_0)$, and the thermoelectric field is given by the temperature gradient,

$$\mathbf{E}_0 = S\boldsymbol{\nabla} T. \tag{13}$$

Inserting this in Gauss' law (5) and using Fourier's equation for heat conduction, we find that the charge density is proportional to the laser intensity,

$$\rho_0(\mathbf{r}) = \frac{\beta\varepsilon S}{\kappa} I(\mathbf{r}). \tag{14}$$

This relation is not surprising but follows directly from the above expression for the thermopotential $\varphi_0(\mathbf{r})$. As a consequence, the charge Q accumulated in the heated spot is proportional to the total absorbed power,

$$Q = \frac{\beta\varepsilon S}{\kappa} \int dV I(\mathbf{r}). \tag{15}$$

III. GAUSSIAN HEATING PROFILE

In many cases the intensity profile of the absorbed laser light is well approximated by a Gaussian of maximum I_0 and width a,

$$I(\mathbf{r}) = I_0 e^{-r^2/a^2}.$$

Then the formal expression (1) for the temperature field is readily integrated,

$$T(\mathbf{r}) - T_0 = \frac{\sqrt{\pi}\beta I_0}{4\kappa r} \operatorname{erf}\left(\frac{r}{a}\right), \tag{16}$$

with Gauss' error function

$$\operatorname{erf}(x) = \frac{2}{\sqrt{\pi}} \int_0^x dt e^{-t^2}.$$

For small x this function increases linearly and rapidly tends toward the limiting value $\operatorname{erf}(\infty) = 1$ for $x > 1$. $T - T_0$ becomes constant at the center of the heated spot, whereas at distances well beyond the beam waist a, the excess temperature decreases as $1/r$.

A. Electric field and thermocharge

The complete expression for the thermoelectric field is obtained by solving (10) and then taking the gradient $E = -\nabla\phi$. We thus obtain

$$E = -S\delta T \frac{a}{r^2} \left[\operatorname{erf}\left(\frac{r}{a}\right) - \frac{1}{2} e^{a^2/4\lambda^2} \times \right. \\ \left. \times \sum_{\pm} \left(\frac{r}{\lambda} \mp 1\right) e^{\pm r/\lambda} \operatorname{erf c}\left(\frac{a}{2\lambda} \pm \frac{r}{a}\right) \right], \tag{17}$$

with the complementary error function $\operatorname{erf c}(x) = 1 - \operatorname{erf}(x)$. In Fig. 2 we plot the thermoelectric field E in units of $S\delta T/a$ as a function of the reduced distance r/a, for different values of the Debye screening length. The five curves are obtained for $\lambda/a = 3; 1; 0.3; 0.1; 0$. The upper one, $(\lambda/a = 0)$ corresponds to $S\nabla T$, that is, the corrections in (17) vanish. At large distances $r \gg a + \lambda$, the electric field is independent of λ, and all curves converge toward $S\nabla T$. Within a volume of radius $a + \lambda$, a significant reduction occurs; as the ratio λ/a increases, the field E becomes smaller than $S\nabla T$.

The charge density is calculated from Gauss' law. From (17) we obtain

$$\rho = \frac{\varepsilon S\delta T a}{2\lambda^2 r} e^{a^2/4\lambda^2} \sum_{\pm} \pm e^{\pm r/\lambda} \operatorname{erf c}\left(\frac{a}{2\lambda} \pm \frac{r}{a}\right). \tag{18}$$

This expression decays exponentially. Total charge (Q) accumulated within and very close to the heated region can be calculate by integrating the charge density and this gives

$$Q = -4\pi a\varepsilon S\delta T_0 = -e(\alpha_+ - \alpha_-)\frac{a}{\ell_B}\frac{\delta T}{T_0}. \tag{19}$$

In the second equality we have used the definition of Bjerrum length $\ell_B = e^2/4\pi\varepsilon k_B T_0$ and expressed the Seebeck coefficient through the ion Soret parameters $\alpha_\pm$. The net charge accumulated is proportional to the excess temperature and to the radius of the heated spot.

B. Limiting case $\lambda/a \to 0$

Most real systems correspond to the limiting case $\lambda \ll a$. Indeed, the size of the heated spot is at least several microns, whereas the Debye length takes values between 1 and 100 nanometers. Then a power series for $\operatorname{erf}(x)$ in terms of $1/x$ provides a useful approximation,

$$\operatorname{erf}(x) = 1 - \frac{e^{-x^2}}{\sqrt{\pi}x}\left(1 - \frac{1}{2x^2} + ...\right).$$

Inserting in the above form for E and retaining the leading terms only, we have

$$E_0 = -S\delta T \frac{a}{r^2}\left(\operatorname{erf}\left(\frac{r}{a}\right) - \frac{2}{\sqrt{\pi}}\frac{r}{a}e^{-r^2/a^2}\right) = S\nabla T. \tag{20}$$

The second equality is readily obtained from the temperature field (16), in accordance with the approximation in

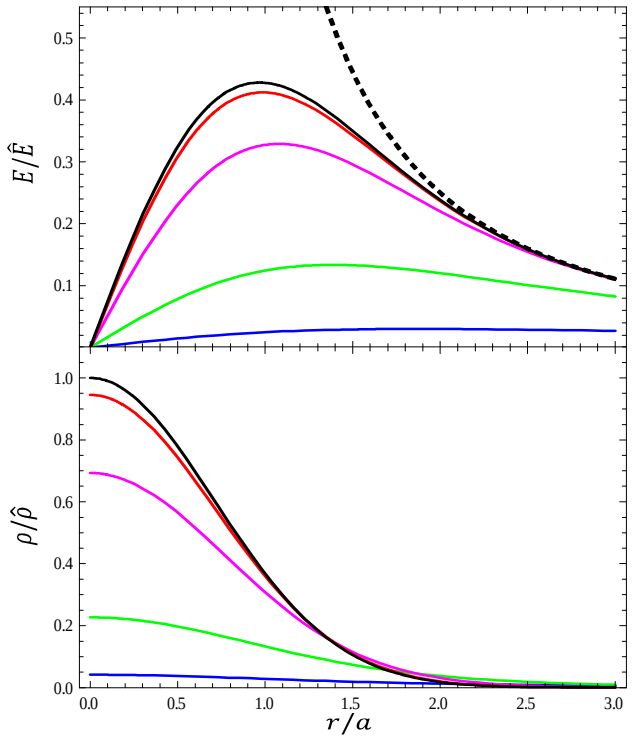

FIG. 2: Upper panel: Thermoelectric field E in units of $\widehat{E} = -S\delta T/a$ as a function of the reduced radial distance r/a. The solid curves are calculated for a Gaussian heating profile; from above they show Eq. (17) with $\lambda/a = 0; 0.1; 0.3; 1; 3$. Thus the top most solid curve corresponds to Eq. (20). The dashed line gives the behavior of the electric field of a point charge, proportional to $1/r^2$. For a hot spot in a NaCl solution of radius $a = 1\mu$m and excess temperature $\delta T = 10$ K, the scale factor takes the value $\widehat{E} = -0.5$ kV/m. Lower Panel: Charge density ρ for Gaussian laser intensity in units of $\widehat{\rho} = -4\varepsilon S\delta T/\sqrt{\pi}a^2$. The curves are calculated from Eq. (18) with the above parameters, resulting in $\widehat{\rho} = -5$ e/μm^3. Except for the upper one, which corresponds to Eq. (21), these curves are not Gaussians; larger values of the ratio λ/a flatten the charge density which approximately covers the domain within $a + \lambda$.

the general case defined in (13). By the same token the charge density (18) simplifies to

$$\rho_0 = -\frac{4\varepsilon S\delta T}{\sqrt{\pi}a^2} e^{-r^2/a^2} = \widehat{\rho} e^{-r^2/a^2}. \qquad (21)$$

As expected from (14), this expression is proportional to the laser intensity. The second equality defines the scale factor for the plots in Fig. 2.

Equations (20) and (21) are plotted in Fig. 2 with the label $\lambda/a = 0$. In the case of finite but small Debye length, these relations provide a very good approximation both inside and outside the heated spot; for $\lambda/a < 0.03$, the error is smaller than the line width in Fig. 2. For a micron-size particle this condition is met for $\lambda < 30$ nm, that is for an electrolyte strength of at least 10^{-4} M/l.

IV. COLLOIDAL TRANSPORT

A. Drift velocity

In recent years local heating with an infrared laser has widely used for confining or sieving macromolecules or colloidal particles in aqueous solution [1, 3–5]. These works rely on the drift velocity u imposed by the temperature gradient. Various physical mechanisms have been discussed [8]; in the present context the most relevant are

$$u = -\frac{\varepsilon\zeta^2}{3\eta}\frac{\nabla T}{T} + \frac{\varepsilon\zeta}{\eta}E, \qquad (22)$$

where ζ is the surface potential, ε the solvent permittivity, and η the viscosity.

In a macroscopic system, the thermoelectric field is strictly proportional to the temperature gradient, $E = S\nabla T$, such that (22) can be rewritten as

$$u_0 = -D_T\nabla T, \qquad D_T = \frac{\varepsilon\zeta^2}{3\eta T} - \frac{\varepsilon\zeta}{\eta}S, \qquad (23)$$

where the thermophoretic mobility D_T is taken as a constant [8]. The first term in D_T arises from the thermoosmotic salt-ion flow around a collodial bead; it was first derived by Ruckenstein [9] and drives the solute particle to the cold. The second term in (22) accounts for electrophoresis in the Seebeck field E. In the last few years it has become clear that this thermoelectric effect contributes significantly to collodial thermophoresis and in many cases is even dominant [16–18]. The velocity may even change its sign with the Seebeck coefficient: This means that negatively charged colloidal particles or SDS micelles move to the warm in NaOH ($S < 0$) and to the cold in NaCl ($S > 0$). As a consequence, the colloid accumulates or is depleted, respectively.

B. Colloidal accumulation at finite radius

For a micron-size hot spot in a very weak electrolyte, the Debye length is of the same order of magnitude of the spot size. Then the thermoelectric properties do not reduce to the macroscopic Seebeck field $E_0 = S\nabla T$ but result in a significantly more involved relation (17) between E and ∇T. As the most striking feature of Fig. 2, moderate or large values of λ/a strongly reduce the thermoelectric field in the heated area, yet are of no effect at larger distances.

In Fig. 3 we plot the spatial variation of the drift velocity u of a colloidal solute in NaOH solution, for different values of the ratio λ/a. Because of the negative Seebeck coefficient of NaOH, the thermoelectric field is opposite to the temperature gradient. Thus for a negatively charged solute, the two terms in (22) carry opposite signs: The Ruckenstein mechanism drives the solute toward the cold, whereas the Seebeck contribution points

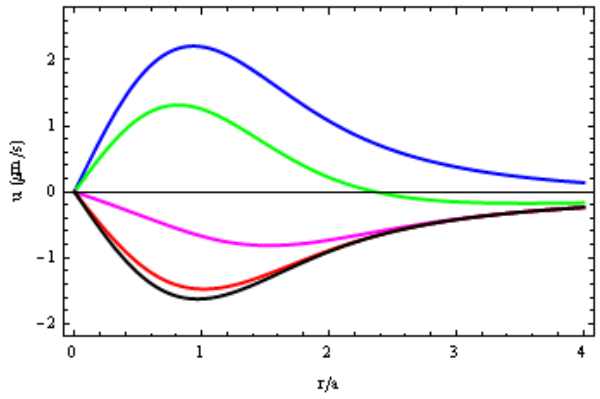

FIG. 3: Spatial variation of the drift velocity (22) for different values of the ratio λ/a. From below the curves are calculated with $\lambda/a = 0; 0.1; 0.3; 1; 3$.

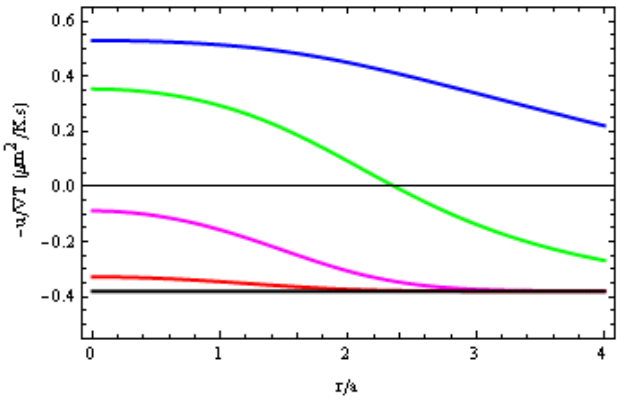

FIG. 4: Spatial variation of the effective thermophoretic mobiltiy $-u/\nabla T$ for different values of the ratio λ/a. From below the curves are calculated with $\lambda/a = 0; 0.1; 0.3; 1; 3$. The lowest one corresponds to the mobility D_T defined in (23)

to the origin of the heated spot. For small λ/a and with the numbers of Table 1, the Seebeck term is dominant everywhere, and the solute migrates to higher temperature ($u < 0$). As the ratio λ/a, increases, the field E decreases below E_0 within the heated area, yet remains unaffected at $r > a+\lambda$ where $E = E_0$. As a consequence, the first term in (22) dominates at at small distances. Accordingly, the solute migrates outward at small r, and in the opposite direction at larger distances; thus the solute accumulates where u vanishes. A similar effect has been shown to result from the competition between thermophoresis and depletion forces [4, 34].

In order to single out the relative variation of the thermoelectric field, we plot in Fig. 4 the ratio of the velocity u and the underlying thermodynamic force ∇T. The lowest curve is calculated with $\lambda/a = 0$, in other words with the Seebeck field $E_0 = S\nabla T$; the constant value $-u/\nabla T = D_T$ gives the usual thermophoretic mobility of the colloid. As λ/a increases, the ratio between u and ∇T is no longer constant, and the thermoelectric contribution is reduced within the heated spot and in its immediate vicinity. For large λ/a and at short distances, the thermoelectric field is negligible and $-u/\nabla T$ tends toward the (positive) value of Ruckenstein contribution in (22). As the distance r increases, the ratio $-u/\nabla T$ changes sign and finally converges to the mobility D_T.

C. Temperature dependence

In the preceding discussion we have assumed that the coefficients of ∇T in (22) and (23) are constant in the heated spot and beyond. It is well known that the properties of both solute and solvent (viscosity, permittivity, Seebeck parameter, ζ-potential) vary with temperature, in addition to the explicit appearance of T in (22). An estimate for real systems shows the largest dependencies occur for the viscosity and Seebeck coefficient; their logarithmic derivatives $d\ln\eta/dT$ and $d\ln S/dT$ are of the order of 0.02 K^{-1} [35], which means that an excess temperature of 10 K results in a change of about 20 percent. There are however, several good reasons for discarding this variation when calculating the drift velocity u.

(i) These corrections are formally similar to those neglected in the linearization approximation of (6). Retaining the former and discarding the latter would be inconsistent. (ii) If the temperature dependence of viscosity and permittivity are rather well known and thus could be taken into account, this is not the case for the Seebeck coefficient S nor for the ζ-potential: There is some evidence that the ionic Soret parameters $\alpha_\pm$, and thus S, are correlated with the thermal expansivity of water [35]; unfortunately there are little data, and a satisfactory theory for the Seebeck coefficient is lacking so far. Regarding the surface potential ζ, its complex temperature dependence is due to the boundary-layer electrostatics and the dissociation of the charged molecular units. In view of these poorly understood dependencies, characterizing the variation of thermoelectric properties with temperature would seem a rather difficult undertaking.

Though not insignificant, these variations are of little relevance for the present discussion, which focusses on the order of magnitude of the thermoelectric effect and on its sign. Thus the coefficients of ∇T in (22) and (23) are calculated with constant $\eta, \varepsilon, S, \zeta$, and T. This is why the mobility D_T, that is, the lowest curve of Fig. 4, does not vary with the distance.

D. Concentration dependence

The drift velocity (22) and (23) has been calculated in the dilute limit, where the Seebeck field E is determined by the salt ions but independent of the colloidal charges. Here a word is in order concerning the back-reaction of

the latter on the thermoelectric properties. In a recent work [19] we have shown that for polyelectrolytes, collective effects set at a volume fraction $\phi \sim \ell_B/R_g$, where $\ell_B = 7$ Å is the Bjerrum length and R_g the gyration radius. A slightly more complex expression occurs for colloidal particles, because of their cooperative diffusion.

Comparison with several experiments suggests that collective effects occur at rather moderately dense suspensions, requiring to go beyond the single-particle picture (22). This is certainly the case in accumulation experiments where thermophoresis contributes to colloidal confinement [36].

V. DISCUSSION

A. Linearization approximation

The analytic results of this paper rely essentially on linearizing the differential equation (6) in terms of excess temperature and modulation of ion densities. Though much higher values can be achieved experimentally [37], typical values for δT are of the order of tens of Kelvin, thus satisfying the first inequality in (7). Regarding the ion densities, a first estimate is obtained by noting that their modulation is of the order $n_\pm - n_0 \sim \alpha_\pm n_0 \delta T/T$; the parameters $\alpha_\pm$ taking values of the order of unity [15], a small excess temperature implies a small change of the ion densities.

Since the thermally induced charge density ρ is a central quantity, we discuss in some detail the fraction ρ/en_0 of salt ions involved. We start with the case of small Debye length $\lambda/a \ll 1$. Inserting the definition $\lambda = (\varepsilon k_B T_0/2e^2 n_0)^{1/2}$ in (21) we find up to a numerical constant

$$\frac{\hat\rho}{en_0} = \frac{eS}{k_B}\frac{\lambda^2}{a^2}\frac{\delta T}{T_0}. \tag{24}$$

According to the numbers of Table I, the first factor on the right-hand side is of the order of unity, which just means $\alpha_\pm \sim 1$. Both of the remaining factors is small however, resulting in $\hat\rho \ll en_0$. As an example, we consider the parameters of Fig. 2 with $\hat\rho = -5e\ \mu\mathrm{m}^{-3}$; for comparison, the ion density of a 1 mM/l electrolyte solution, $n_0 = 6\times 10^5\ \mu\mathrm{m}^{-3}$, is by five orders of magnitude larger than the net charge density. For the case where the Debye length exceeds the size of the hot spot, $\lambda > a$, one finds a relation similar to (24), albeit without the factor λ^2/a^2. Again, for typical excess temperatures $\delta T \sim 10$K, the net charge density turns out to be by almost two orders of magnitude smaller than salinity. Thus the inequality

$$\rho \ll en_0$$

holds independently of the ratio λ/a. This means that thermal charge separation involves only a small fraction of the ion density.

On the other hand, this inequaltiy implies the second relation of (7). Writing the charge density as $\rho = e(n_+ - n_0) - e(n_- - n_0)$ and noting that it is dominated by the ion species with the larger heat of transfer parameter $\alpha_\pm$, for example $\rho \approx -e(n_- - n_0)$ in the case of NaOH ($\alpha_+ = 0.7$ and $\alpha_- = 3.4$), we find that $|\rho| \ll en_0$ implies the concentration change of both cations and anions to be small. These estimates confirm the validity of the linearization approximation for the fundamental equation (6). Since experimental studies of confinement, separation, and transport, hardly exceed an excess temperature δT of 15 K, the thermoelectric properties should be well described by the present work. The smooth functional behavior of Eq. (6) suggests that our qualitative results hold true even at much larger excess temperature $\delta T \sim T$, where $\hat\rho/en_0 \sim \lambda^2/a^2 \ll 1$.

B. Thermocharge and Seebeck field

The main results of the present work are the thermocharge Q accumulated in the heated spot, and the corresponding electric field E. According to Eq. (19) the charge is proportional to the reduced Seebeck parameter $\alpha_+ - \alpha_-$, to the size of the spot in units of the Bjerrum length $\ell_B = 0.7$ nm, and to the reduced excess temperature. For a spot of $a = 5\mu$m radius and excess temperature $\delta T = 30$ K, the induced Q takes a value of about thousand elementary charges.

At distances well beyond the heated spot, $r \gg a$, the thermoelectric field takes the form

$$E = \frac{Q}{4\pi\varepsilon r^2}. \tag{25}$$

The variation with the inverse square of the distance, characteristic of an unscreened field, highlights the fact that the heated spot carries a net charge Q. The field takes its maximum value at $r \sim a$; with the above parameters, it is of the order of kV/m.

The ratio of the Debye length λ and the size of the hot spot a turns to be an important parameter. For $\lambda \ll a$ we find that the thermo-charge density ρ is proportional to the heating power, as shown in (14) for the general case and in (21) for a Gaussian heating profile. A more complex situation occurs if λ is not small as compared to the size of the heated domain. The lower panel of Fig. 2 shows that already at $\lambda/a = \frac{1}{3}$ the charge density in the center is reduced by one third, and augmented at large distances accordingly. As a consequence of this smearing out of the thermocharge, the electric field is reduced within and in the vicinity of the heated area; at larger distances E tends towards (25).

C. Thermally driven convection

So far we have neglected convection induced in the liquid by the temperature gradient. Because of the thermal

expansion, the heated spot has a slightly lower density. Thus gravity drives an upward convective flow, similar to the Rayleigh-Bénard cells that develop in a horizontal layer of fluid heated from below. An estimate of velocity is obtained by equilibrating the buoyancy and Stokes drag forces [38],

$$u_c \sim \beta \delta T g a^2/\nu,$$

with the thermal expansivity $\beta = 2\times10^{-4}$ K^{-1} and kinematic viscosity $\nu = 10^{-6}$ m^2/s of water at room temperature. For a heated spot of size $a = 10\mu$m and excess temperature $\delta T = 10$ K one finds a convective velocity u_c of about 10 μm/s.

An important question is whether or not the mobile charges are advected by this flow. This is best answered in term of the Péclet number,

$$\mathrm{Pe} = \frac{u_c}{D/a},$$

that compares the convection velocity with diffusion over the characteristic length a. With the Einstein coefficient of common ions $D = 2\times10^{-9}$ m^2/s and $a = 10\mu$m, one finds $D/a = 200$ μm/s and a Péclet number of about 5%. In physical terms this means that the salt ions diffuse sufficiently rapidly, such that the charge profile ρ and the thermoelectric field E are hardly affected by convection.

A different picture arises for a colloidal suspension. Because of the much smaller Einstein coefficient, $D = 2\times10^{-12}$ m^2/s for 100 nm beads, the Péclet number is larger than unity and diffusion is much slower than advection [38]. The interplay between diffusion, convection, and thermophoresis has been used in thermal traps and separation devices [1, 4].

Finally we note that the present work deals with a stationary temperature profile. Additional flows arise from time-dependent heating, as illustrated by experiments using thermoviscous expansion [39].

D. Non-spherical geometries

We conclude with a brief discussion of non-spherical geometries. In most cases the laser intensity $I(\mathbf{r})$ has no spherical symmetry, that is, it shows different profiles parallel and perpendicular to the beam axis, and so does the excess temperature. Then (9) and (10) do not reduce to a single radial equation. Still, if the spatial variation of T is slow on the scale of the Debye length, $\lambda|\nabla T| \ll \delta T$, the thermoelectric field follows the temperature gradient according to the macroscopic law $E_0 = S\nabla T$. As an important result, Eqs. (13) and (14) are valid for any sufficienlty smooth heating profile; this implies in particular the existence of the thermocharge (19), with some characteristic length a.

Thus the analysis of Sect. 2 is valid for any smooth temperature profile. The results obtained in Sects 3 and 4, however, and in particular the electric field (17) and the thermophoretic velocity (23), rely on the spherical symmetry of both thermal and electric properties. Significant deviations occur for a non-spherical heated spot that is not much larger than the Debye length, or for an electrolyte that is confined by a solid boundary. We briefly discuss the latter situation.

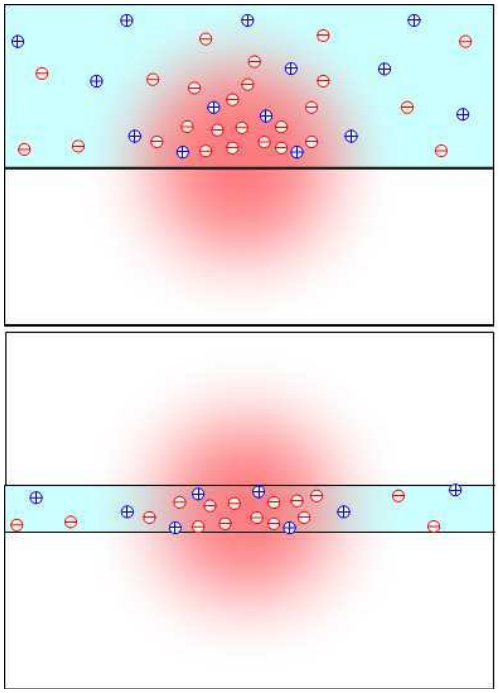

FIG. 5: Heated spot at a liquid-solid boundary (upper panel) or in thin aqueous film (lower panel).

We consider a confined electrolyte solution, where the ratio of the permittivities of water ε and the insulating boundary $\varepsilon_{\mathrm{in}}$ constitutes a most important parameter; for typical materials one has $\varepsilon/\varepsilon_{\mathrm{in}} \sim 30$. The upper panel of Fig. 5 shows a heated spot at a liquid-solid or liquid-liquid interface. Though this geometry does not allow for a general solution of the thermoelectric equations, qualitative features are readily obtained by comparing with results for a discrete surface charge Q [40]. Estimating the ion pressure and the Maxwell stress tensor $\mathcal{T}$ in the framework of Debye-Hückel theory, one finds a normal stress component $\mathcal{T} \sim Q^2/\varepsilon_{\mathrm{in}}a^4$ that pushes the interface toward the electrolyte; the resulting force on the heated spot, $F \sim Q^2/\varepsilon_{\mathrm{in}}a^2$, is counterbalanced by the opposite stress on the outside area [41]. This thermoelectric stress could contribute to the temperature-driven forces on droplets that are used for optothermal actuation in microfluidic devices [2].

Even more striking effects are expected to occur in a locally heated thin aqueous film, as illustrated in the lower panel of Fig. 5. The ratio of the film thickness h and the size a of the hot spot provide an important parameter for the thermoelectric equations. For $h \gg a$ one recovers the bulk behavior studied in this paper, whereas a rather

different picture arises in the opposite case $h < a$. The permittivity jump at the interfaces confines the electric field lines and results in a strongly non-uniform relation between E and ∇T, similar to that discussed above for the ratio λ/a. According to our preliminary results, this confinement could be relevant for the thermophoretic mobility observed for thin-film geometries [4, 22, 42].

VI. SUMMARY

We briefly summarize our main results on the thermoelectric properties of a locally heated spot in an electrolyte solution.

(i) For a smooth temperature profile, that varies little within one Debye length, the Seebeck field (13) and the thermocharge density (14) are proportional to the temperature gradient and laser intensity, respectively. These results does not rely on a particular geometry but hold true in general.

(ii) The total charge (15) is proportional to the integrated power. With typical experimental parameters, Q may attain thousand elementary charges.

(iii) Laser heating can be used for designing local electric fields of the order of kV/m, without electrodes or other material in the electrolyte solution. This thermoelectric field is not screened and, beyond the heated spot, decays with the square of the inverse distancė.

(iv) In recent years, thermal gradients have been used for accumulating or depleting colloidal solutes in a hot spot. The Seebeck field derived here could contribute significantly to the thermodynamic forces observed experimentally, and provide an qualitative picture for situations where convection is of little relevance, for example in confined micron-size films. Regarding thermoconvection, which is present in a bulk system, we find that salt ions are hardly affected (small Péclet number), whereas the stationary state of colloidal solutes is to a large extent determined by advection.

[1] S. Duhr and D. Braun, *Phys. Rev. Lett.*, 2006, **97**, 038103.
[2] C. Baroud, J.-P. Delville, F. Gallaire and R. Wunenburger, *Phys. Rev. E: Stat., Nonlinear, Soft Matter Phys.*, 2007, **75,** 046302.
[3] H.-R. Jiang, H. Wada, N. Yoshinaga and M. Sano, *Phys. Rev. Lett.*, 2009, **102**, 208301.
[4] Y.T. Maeda, A. Buguin and A. Libchaber, *Phys. Rev. Lett.*, 2011, **107**, 038301.
[5] C.J. Wienken, Ph. Baaske, U. Rothbauer, D. Braun and S. Duhr, *Nature Communications*, 2010, **1**, 100.
[6] S. Wiegand, J. Phys. Cond. Matt. **16**, 357 (2004)
[7] R. Piazza, *Soft Matter*, 2008, **4**, 1740.
[8] A. Würger, *Rep. Prog. Phys.*, 2010, **73**, 126601.
[9] E. Ruckenstein, *J. Coll. Interf. Sci.*, 1981, **83**, 77.
[10] R.M. Muruganathan, Z. Khattari and Th. M. Fischer, *J. Phys. Chem. B*, 2005, **109**, 21772.
[11] F. Bresme, A. Lervik, D. Bedeaux, and S. Kjelstrup, *Phys. Rev. Lett.*, 2008, **101**, 020602.
[12] F. Römer, F. Bresme, J. Muscatello, D. Bedeaux and J. Miguel Rubı, *Phys. Rev. Lett.*, 2012, **108**, 105901.
[13] E. D. Eastman, *J. Am. Chem. Soc.*, 1928, **50**, 292-297.
[14] G. Guthrie, J. N. Wilson and V. Schomaker, *J. Chem. Phys.*, 1949, **17**, 310-313.
[15] J. N. Agar, C. Y. Mou and J.-L. Lin, *J. Phys. Chem.*, 1989, **93**, 2079-2082.
[16] S.A. Putnam and D.G. Cahill., *Langmuir*, 2005, **21**, 5317.
[17] D. Vigolo, S. Buzzaccaro and R. Piazza, *Langmuir*, 2010, **26**, 7792.
[18] A. Würger, *Phys. Rev. Lett.*, 2008, **101**, 108302.
[19] A. Majee and A. Würger, *Phys. Rev. E: Stat., Nonlinear, Soft Matter Phys.*, 2011, **83**, 061403.
[20] N. Ghofraniha, G. Ruocco and C. Conti, *Langmuir*, 2009, **25**, 12495.
[21] S. Iacopini, R. Rusconi, and R. Piazza, *Eur. Phys. J. E*, 2006, **19**, 59-67.
[22] S. Duhr and D. Braun, *Proc. Natl. Acad. Sci. USA*, 2006, **103**, 19678-19682.
[23] K.. Eslahian and M. Maskos, *Colloids and Surfaces A*, 2012
[24] R. W. O'Brian and L. R. J. White, *J. Chem. Soc. Faraday Trans. II.*, 1978, **74**, 1607.
[25] M. Antonietti and L. Vorwerg, *Colloid Polym Sci.*,1997, **275**, 883.
[26] D. Lüsebrink, M. Ripoll, J. Chem. Phys. 136, 084106 (2012)
[27] D. Lüsebrink, M. Yang, M. Ripoll, J. Phys.: Condens. Matter **24**, 284132 (2012)
[28] A. Majee and A. Würger, *Phys. Rev. Lett.*, 2012, **108**, 118301.
[29] P.C. Hiemenz, R. Rajagopalan, *Principles of Colloid and Surface Chemistry*, Dekker (1997)
[30] J.O. Anderson, *Ann. Rev. Fluid Mech.* 1989, **21**, 61.
[31] S.R. de Groot and P. Mazur, *Non-equlibrium thermodynamics*, North Holland Publishing, Amsterdam, 1962.
[32] V. N. Sokolov, L. P. Safonova and A. A. Pribochenko, *J. Solution Chem.*, 2006, **35**, 1621.
[33] M. Bonetti, S. Nakamae, M. Roger and P. Guenoun, *J. Chem. Phys.*, 2011, **134**, 114513.
[34] K. Odagiri, K. Seki and K. Kudo, *Soft Matter* 2012, **8**, 6775-6781.
[35] A. Würger, *Langmuir* 2009, **25**, 6696-6701.
[36] D. Braun and A. Libchaber, *Phys. Rev. Lett.*, 2002, **89**, 188103.
[37] D. Rings, R. Schachoff, M. Selmke, F. Cichos, K. Kroy, *Phys. Rev. Lett.* 2010, **105**, 090604.
[38] R. Rusconi, L. Isa, R. Piazza, *J. Opt. Soc. Am.* 2004, **21**, 605
[39] F.M. Weinert, D. Braun, *J. Appl. Phys.* 2008, **104**, 104701
[40] L. Foret, R. Kühn, A. Würger, *Phys. Rev. Lett.* 2002, **89**, 156102.
[41] L. Foret, A. Würger, *Phys. Rev. Lett.* 2004, **92**, 058302.
[42] H.-R. Jiang, N. Yoshinaga, M. Sano, *Phys. Rev. Lett.*,

2010, **105**, 268302.